Acta Biomaterialia 9 (2013) 4906–4915

Contents lists available at SciVerse ScienceDirect

Acta Biomaterialia

journal homepage: www.elsevier.com/locate/actabiomat

Osteogenic and angiogenic potentials of monocultured and co-cultured human-bone-marrow-derived mesenchymal stem cells and human-umbilical-vein endothelial cells on three-dimensional porous beta-tricalcium phosphate scaffold

Yunqing Kang [a], Sungwoo Kim [a], Monica Fahrenholtz [b], Ali Khademhosseini [c,d,e], Yunzhi Yang [a,*]

[a] Department of Orthopedic Surgery, Stanford University, 300 Pasteur Drive, Stanford, CA 94305, USA
[b] Department of Bioengineering, Rice University, 6100 Main St., Houston, TX 77030, USA
[c] Center for Biomedical Engineering, Department of Medicine, Brigham and Women's Hospital, Harvard Medical School, Cambridge, MA 02139, USA
[d] Harvard-MIT Division of Health Sciences and Technology, Massachusetts Institute of Technology, Cambridge, MA 02139, USA
[e] Wyss Institute for Biologically Inspired Engineering, Harvard University, Boston, MA 02115, USA

ARTICLE INFO

Article history:
Received 14 April 2012
Received in revised form 23 July 2012
Accepted 8 August 2012
Available online 16 August 2012

Keywords:
β-TCP
hBMSCs
HUVECs
Osteogenesis
Angiogenesis

ABSTRACT

The use of biodegradable beta-tricalcium phosphate (β-TCP) scaffolds holds great promise for bone tissue engineering. However, the effects of β-TCP on bone and endothelial cells are not fully understood. This study aimed to investigate cell proliferation and differentiation of mono- or co-cultured human-bone-marrow-derived mesenchymal stem cells (hBMSCs) and human-umbilical-vein endothelial cells (HUVECs) on a three-dimensional porous, biodegradable β-TCP scaffold. In co-culture studies, the ratios of hBMSCs:HUVECs were 5:1, 1:1 and 1:5. Cellular morphologies of HUVECs, hBMSCs and co-cultured HUVECs/hBMSCs on the β-TCP scaffolds were monitored using confocal and scanning electron microscopy. Cell proliferation was monitored by measuring the amount of double-stranded DNA (dsDNA) whereas hBMSC and HUVEC differentiation was assessed using the osteogenic and angiogenic markers, alkaline phosphatase (ALP) and PECAM-1 (CD31), respectively. Results show that HUVECs, hBMSCs and hBMSCs/HUVECs adhered to and proliferated well on the β-TCP scaffolds. In monoculture, hBMSCs grew faster than HUVECs on the β-TCP scaffolds after 7 days, but HUVECs reached similar levels of proliferation after 14 days. In monoculture, β-TCP scaffolds promoted ALP activities of both hBMSCs and HUVECs when compared to those grown on tissue culture well plates. ALP activity of cells in co-culture was higher than that of hBMSCs in monoculture. Real-time polymerase chain reaction results indicate that *runx2* and *alp* gene expression in monocultured hBMSCs remained unchanged at days 7 and 14, but *alp* gene expression was significantly increased in hBMSC co-cultures when the contribution of individual cell types was not distinguished.

1. Introduction

Tissue engineering holds great promise for regenerating functional tissues and organs. One important component of tissue engineered materials is the scaffold, which is an artificial extracellular matrix (ECM) that serves as a temporary support structure and imparts the necessary biophysical, biomechanical and biochemical cues required for cell attachment, proliferation and differentiation to form tissue [1]. In particular, it is highly desirable for scaffolds to possess an interconnected and open macroporous structure to facilitate cellular in-growth and neovascularization of regenerated tissue in vivo.

Calcium phosphate (CaP) bioceramics have been widely used in clinical settings for bone repair and reconstruction [2,3]. Hydroxyapatite (HA) and beta-tricalcium phosphate (β-TCP) are the most popular bioceramics due to their close resemblance to natural bone, excellent biocompatibility and biodegradability. Bone-marrow-derived mesenchymal stem cells (BMSCs) have been used in combination with CaP scaffolds in bone tissue engineering [4–7]. Many studies involving the use of BMSC-seeded bioceramics have shown promising results in the context of bone regeneration [8–11]; however, most of these investigations have highlighted the osteogenic potential of BMSCs on these CaP bioceramics.

Bone tissue contains multiple cell types, including osteogenic cells and endothelial cells. A number of studies in bone repair and regeneration have highlighted the intimate interactions

* Corresponding author. Tel.: +1 650 723 0772; fax: +1 650 724 5401.
E-mail address: ypyang@stanford.edu (Y. Yang).

1742-7061/$ - see front matter © 2012 Acta Materialia Inc. Published by Elsevier Ltd. All rights reserved.
http://dx.doi.org/10.1016/j.actbio.2012.08.008

between endothelial cells and osteoprogenitor cells [12,13]. Indeed, it has been well established that angiogenesis is a prerequisite for osteogenesis in vivo [14]. For example, insufficient neovascularization of bone constructs/tissues after scaffold implantation resulted in hypoxia and cellular necrosis [15–19]. Thus, a key factor in repairing large bone defects is vascularization of the scaffold. Within this context, it is important to characterize the effects of bioceramic scaffolds with regards to osteogenic and endothelial differentiation. It has been reported that co-cultured human endothelial cells with human osteoblast cells on porous HA, β-TCP or Ca-deficient HA containing polycaprolactone supported the formation of capillary-like structures [20,21]. Zhou et al. pre-vascularized β-TCP scaffold by co-seeding MSCs and MSC-derived endothelial cells (ECs) and used it to promote the repair of segmental bone defects in rabbits [22].

In this study, we investigated the effect of a porous, biodegradable β-TCP scaffold on the behavior of mono- or co-cultured human-bone-marrow-derived mesenchymal stem cells (hBMSCs) and human-umbilical-vein endothelial cells (HUVECs). We hypothesize that different cell ratios of hBMSCs and HUVECs may behave differently on a porous, biodegradable β-TCP scaffold. In this experiment, interconnected porous β-TCP scaffolds were prepared by a template-casting method [23–25]. Cell proliferation was monitored by measuring the amount of double-stranded DNA (dsDNA), whereas hBMSC and HUVEC differentiation was assessed using the osteogenic and angiogenic markers alkaline phosphatase (ALP) and PECAM-1 (CD31), respectively.

2. Materials and methods

2.1. Materials

β-TCP powder with a specific surface area of 17 $m^2 g^{-1}$ was purchased from Nanocerox, Inc. (Ann Arbor, Michigan). Carboxymethyl cellulose powder, paraffin beads and ethyl alcohol were purchased from Fisher Scientific (Pittsburgh, USA).

Dulbecco's modified Eagle's medium (DMEM), fetal bovine serum (FBS) and L-glutamine, 100 × antibiotic–antimycotic solution were purchased from Invitrogen Co. (Grand Island, NY, CA). EBM™ endothelial basal medium containing EGM™ endothelial growth medium and a Single Quots™ kit were purchased from Lonza, Inc. Alexa Fluor® 594 goat anti-mouse secondary antibody (2 mg ml^{-1}) was purchased from Invitrogen Inc. An RNeasy mini kit for extracting RNA was purchased from QIAGEN (Valencia, CA, USA).

2.2. Preparation of β-TCP scaffolds

Porous β-TCP scaffolds were fabricated using a template-casting method as previously described [23–25]. Briefly, β-TCP powder, carboxymethyl cellulose powder, surfactant (Surfonal®) and dispersant (Darvan® C) were mixed in distilled water to form a ceramic slurry. Paraffin beads were packed into a customized mold and heated to induce partially melting and formation of a template. The β-TCP ceramic slurry was then cast into the mold under vacuum, solidified and subsequently dehydrated in a series of ethyl alcohol solutions (70%, 90% and 95%). After removing the dehydrated green body from the mold, the green body was dried in an oven for 2 h, and then placed into an electric high temperature furnace and sintered at 1250 °C for 3 h. The morphology of β-TCP scaffolds was characterized by scanning electron microscopy. The average pore size of scaffold was obtained from scanning electron microscopy (SEM) images and at least six pores were measured. The interconnected pore structure of scaffold was scanned using micro-computed tomography (micro-CT; Imtek Micro CAT II, Knoxville, TN) at a resolution of 80 μm. Raw images were further reconstructed and analyzed by GE microView software (General Electric Co.). The scaffolds used in this study were 7–8 mm in diameter and 5–6 mm in height.

2.3. Cell culture of hBMSCs and HUVECs

hBMSCs were purchased from Lonza Inc. (Allendale, NJ) [26]. According to the manufacturer's certificate of analysis, the cells are more than 90% positive for CD105, CD166, CD29 and CD44, and less than 10% positive for CD14, CD34 and CD45. The cells were cultured in basal medium consisting of DMEM, (Invitrogen, USA) with 10% FBS, 1% L-glutamine (200 mM) and 1% antibiotic–antimycotic solution under standard conditions (5% CO_2, 95% humidity, and 37 °C). Passages 6–8 were used for all the experiments.

Immortalized HUVECs constitutively expressing green fluorescent protein (GFP) were a generous gift from the late Dr. J. Folkman, Children's Hospital, Boston. HUVECs were cultured in endothelial basal medium (EBM-2, Lonza) with endothelial growth supplement Single Quots (EGM-2, Lonza) in a 5% CO_2 atmosphere at 37 °C.

A preliminary study was performed to test the culture medium for co-culture experiments (Supplementary Fig. S1). In this study, the medium used in all co-culture experiments was a 1:1 mixture of EBM-2 and DMEM.

When the cells reached ~85–90% confluence in flasks, they were subcultured using 0.25% trypsin–EDTA (Invitrogen, USA) and resuspended in culture medium. Next, 100,000 cells in 100 μl medium were gently seeded into the sterilized β-TCP scaffolds and incubated at 37 °C for 1 h to allow cells to attach onto the inner construct surface of the scaffold. New medium was then added for further incubation. The medium was changed every 3 days. To investigate the reciprocal effect of the two cell types on osteogenesis and angiogenesis, three mixture ratios (1:5, 1:1, 5:1) of hBMSCs and HUVECs were seeded and co-cultured on the scaffolds. In mono- and co-culture experiments, the seeding density (100,000 cells per scaffold) was held constant regardless of cell mixture ratios. To indicate the cell distribution in the scaffolds, scaffolds with seeded HUVEC-GFP cells were recaptured using a fluorescent microscope (Nikon 2000) and shown in Supplementary Fig. S2.

2.4. Morphologies of HUVECs, hBMSCs and co-cultured cells on the β-TCP scaffolds

The morphology of HUVECs on β-TCP scaffolds was monitored using a confocal laser scanning microscope (CLSM; Olympus IX81) after 1, 3 and 7 days of incubation in EBM-2 medium. Morphologies of HUVECs, hBMSCs and hBMSC/HUVEC mixtures seeded on the β-TCP scaffolds were also observed under a scanning electron microscope (SEM, FEI Quanta 400). HUVECs and hBMSCs in monoculture were incubated in EBM-2 and DMEM, respectively, and hBMSC/HUVEC mixture cells (50%:50%) were co-cultured in EBM-2:DMEM mixture medium (1:1) for 3 days. Following this, scaffolds were fixed with 2.5% glutaraldehyde for 2 h, followed by graded dehydration using a series of ethanol solutions (generally 70%, 80%, 90% and 100%). Samples were then dried in a hood and sputtered with gold before observation under an SEM (FEI Quanta 400) at 20 kV.

2.5. Visualization of F-actin

F-actin was stained by rhodamine phalloidin to assess cytoskeletal organization on the β-TCP scaffold. After 7 days of incubation in the same medium as used in the experiments for SEM, cells/scaffolds were rinsed twice using phosphate buffered saline (PBS) and then fixed by 4% paraformaldehyde solution (PFA) for 15 min at room temperature. The fixed cells were further permeabilized in

0.5% Triton X-100 and incubated in 100 nM rhodamine phalloidin working solution (Cytoskeleton Inc., USA) at room temperature for 2 h. After a brief rinse with PBS, DAPI solution (5 μg ml^{-1}) was added to counterstain cell nuclei. After a thorough washing with PBS, cells on scaffolds were visualized with a CLSM.

2.6. Immunofluorescent staining of PECAM-1

Platelet-endothelial cell adhesion molecule (PECAM-1, or CD31) is an endothelial-specific adhesion protein and a specific marker of HUVECs. It was assessed by immunefluorescent staining. The effect of β-TCP scaffolds on PECAM-1 expression of HUVECs in monoculture or co-culture with hBMSCs in various ratios (1:5, 1:1, 5:1) were investigated at 7 and 14 days. They were cultured in a 1:1 mixture of EBM-2 and DMEM, and then rinsed twice with PBS and fixed in a solution of 4% PFA for 15 min at room temperature. After washing three times in PBS, the fixed cells/scaffolds were placed in 3% bovine serum albumin (BSA)/PBS blocking buffer for 1 h, and then were incubated with mouse anti-human CD31 primary antibody (1:3000, Cell Signaling Technology) in 1% BSA/PBS overnight at 4 °C. The cells/scaffolds were then washed three times using PBS, and incubated in an anti-mouse secondary antibody Alexa Fluor®594 (1:1000; 2 μg ml^{-1}, Invitrogen) for 1 h at room temperature. After a brief rinse using PBS, the cell nuclei were counterstained with DAPI solution (5 μg ml^{-1}) for 1 min. The scaffold samples were then extensively washed with PBS, and visualized with a CLSM.

2.7. Osteogenic differentiation assay of hBMSCs

The effect of β-TCP scaffolds on the early osteogenic differentiation of hBMSCs in monoculture and co-culture was assessed through ALP specific activity. hBMSCs were co-cultured with various ratios of HUVECs (5:1, 1:1, 1:5) on the scaffolds. Monocultured hBMSCs and HUVECs were used as controls. The medium used in these co-culture experiments was a 1:1 mixture of EBM-2 and DMEM, as determined in our preliminary study (S.1).

At the end of each time point, cells/scaffolds were washed twice with PBS and preserved at −80 °C. Cells/scaffolds experiencing three freeze/thaw cycles in −80 °C/37 °C, were then lysed in 500 μl of 0.2% Triton X-100 in PBS, and finally homogenized by sonication for 30 s on ice. The ALP activity was assayed using a colorimetric p-NPP method [23,24]. The absorbance was measured on a microplate reader (TECAN) at 405 nm after 30 min incubation at 37 °C. ALP specific activity levels were quantified with a standard curve and normalized to the amount of total cellular dsDNA from the same sample. dsDNA content was determined using a Pico Green assay (Molecular Probe, Invitrogen). A 50 μl volume of working reagent was added to the 50 μl cell lysate of the sample. The sample was read at 485/528 nm (excitation/emission) on a fluorescence spectrophotometer (Biotek, Flx800, USA). The amount of dsDNA was calculated by comparing the standard curves of the known dsDNA sample according to the manufacturer's instruction.

2.8. Quantitative real-time polymerase chain reaction (PCR)

Total RNA of cells was extracted from the monocultured and co-cultured cells after incubation of 7 and 14 days using an RN easy mini Kit (QIAGEN) following the manufacturer's protocol. RNA concentration was determined on an Eppendorf Biophotometer. To reverse-transcribe RNA of the samples into cDNA, an iScript cDNA synthesis kit (BIO-RAD) was used according to the manufacturer's protocols. Using cDNA product template, specific primers and iQ-SYBR Green supermix (BIO-RAD), real-time PCR was performed on an ABI 7900HT Sequence Detection system (ABI, Foster city, USA). The total reaction volume was 10 μl. Primer sequences are shown in Table 1, including runt-related transcription factor 2 (*runx2*), alkaline phosphatase (*alp*), osteopontin (*opn*), osteocalcin (*oc*), bone sialoprotein (*bsp*), bone morphogenetic protein-2 (*bmp-2*), *cd31* and glyceraldehyde 3-phosphate dehydrogenase (GAPDH). These primers were purchased from Invitrogen Co. and used to evaluate gene expression [27–29]. The relative expression levels of genes were analyzed using the $2^{-\Delta\Delta Ct}$ method [30] by normalizing with the housekeeping gene GAPDH as an endogenous control and calibrating with efficiency, where ΔΔCt is calculated from $(C_{t,\ target} - C_{t,\ control})_{target\ gene} - (C_{t,\ target} - C_{t,\ control})_{GAPDH}$.

Table 1
Sequences of primers used for real-time PCR analysis.

Genes	Sequences
GAPDH	For: 5′-AACAGCGACACCCACTCCTC Rev: 5′-CATACCAGGAAATGAGCTTGACAA
runx-2	For: 5′-AGATGATGACACTGCCACCTCTG Rev: 5′-GGGATGAAATGCTTGGGAACT
alp	For: 5′-ACATTCCCACGTCTTCACATTT Rev: 5′-AGACATTCTCTCGTTCACCGCC
opn	For: 5′-ATGAGATTGGCAGTGATT Rev: 5′-TTCAATCAGAAACTGGAA
oc	For: 5′-TGTGAGCTCAATCCGGACTGT Rev: 5′-CCGATAGGCCTCCTGAAGC
bsp	For: 5′-ATGGCCTGTGCTTTCTCAATG Rev:5′-GGATAAAAGTAGGCATGCTTG
bmp-2	For:5′-GCCCTTTTCCTCTGGCTAT Rev:5′-TTGACCAACGTCTGAACAATGG
cd31	For: 5′-GAGTCCTGCTGACCCTTCTG Rev: 5′-CACTCCTTCCACCAACACCT

2.9. Statistical analysis

All the groups in the experiments were performed in triplicate, and the statistical significance was analyzed by Student's *t*-test. If the *p*-values obtained from the *t*-test were less than 0.05, the difference was considered to be significant.

3. Results

3.1. Porous morphologies of the β-TCP scaffold

Representative morphology of a β-TCP scaffold is shown in Fig. 1. The porous structure and interconnected pores of a β-TCP scaffold is shown in Fig. 1A at a lower magnification. The pores size of the scaffold is in the range of 350–500 μm and the average pore size measured from SEM images is ∼396 ± 49 μm. Fig. 1B indicates a local strut of the scaffold at a higher magnification. The strut surface appears dense and consists of microscale grains. Fig. 1C–E shows the representative three-dimensional (3-D) and two-dimensional (2-D) reconstructed micro-CT images. The interconnected pores are observed across the scaffold in Fig. 1C–E.

3.2. Cell morphologies on the β-TCP scaffold

Morphologies of GFP-tagged HUVECs on the β-TCP scaffold were observed with a CLSM. Fig. 2 shows cell morphology changes on a β-TCP scaffold over time. Fluorescent images in Fig. 2A show that HUVECs adhered and spread well on the surface of struts and inner pores of the scaffold at day 1, and cells exhibited a cobblestone-like morphology. HUVECs proliferated well on the scaffold with increasing culture time. At day 3, HUVECs covered the majority of the strut surface (Fig. 2B) and a dense endothelial layer was formed by day 7 (Fig. 2C). In this study, SEM was used to

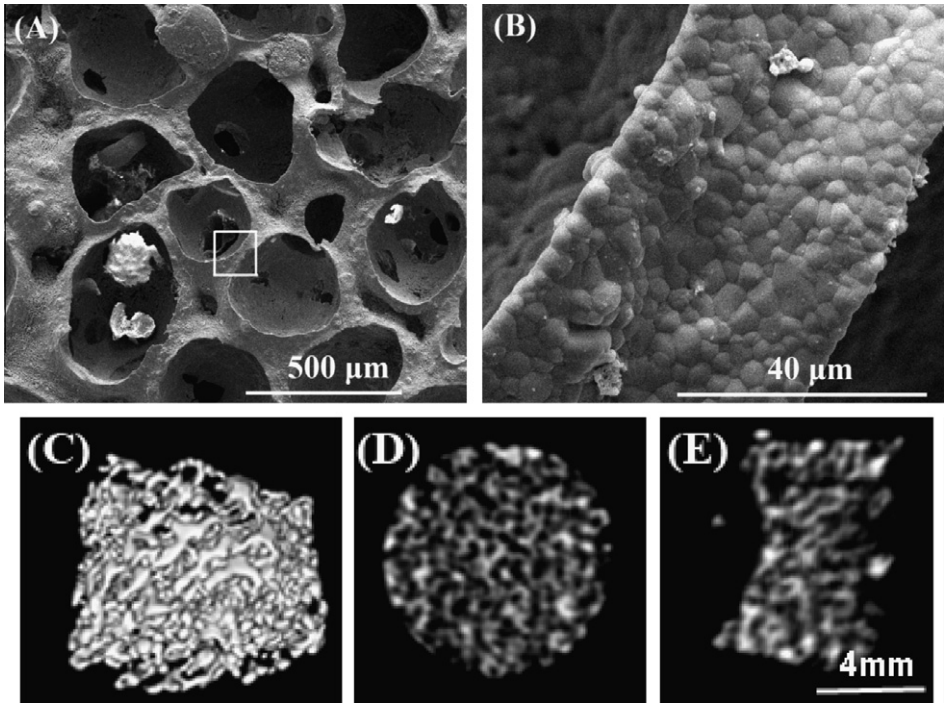

Fig. 1. SEM morphologies of the β-TCP scaffold with different magnifications: (A) interconnected pores at low magnification (50×), and (B) the local strut surface at high magnification of the square area in (A) (3000×). Micro-CT images indicate the interconnected pores of scaffold in 3-D (C), and 2-D reconstruction (D) and (E).

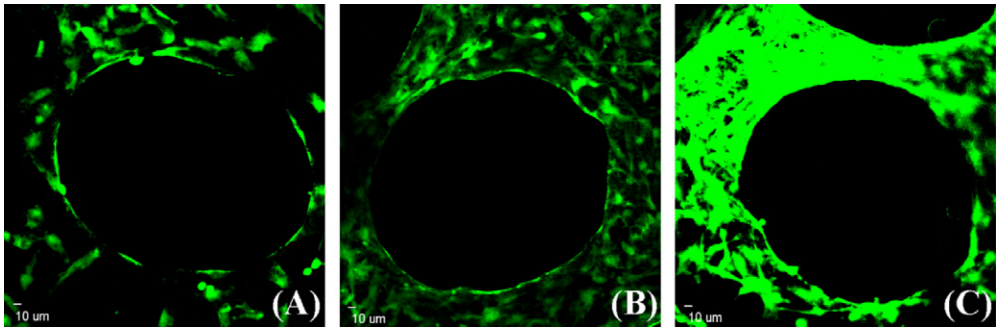

Fig. 2. HUVEC adhesion and spread morphology on the struts of a β-TCP scaffold observed by confocal laser scanning microscopy. HUVECs are observed to attach and grow well on the scaffold for (A) 1 day, (B) 3 days and (C) 7 days. Images were captured on the same site of one scaffold.

further investigate cell morphologies of hBMSCs and HUVECs on the β-TCP scaffolds. Results showed that both hBMSCs and HUVECs can adhere well on the scaffolds (Fig. 3). In monocultures, HUVECs exhibited cobblestone-like morphology and formed a flattened endothelial cell layer (Fig. 3A), while hBMSCs exhibited a typical spindle-like morphology (Fig. 3B). In co-culture of hBMSCs and HUVECs, both spindle-like cells and cobble-like cells could be observed, suggesting the co-existence of both cell types on the scaffold (Fig. 3C).

3.3. Visualization of F-actin filament of cells

In HUVEC and hBMSC monocultures, an abundance of actin fibers was observed in the cytoplasm of the cells (Fig. 4A, G and C, H). The fluorescent image in Fig. 4B shows cobblestone-like morphology. In hBMSC monocultures, the rhodamine phalloidin/DAPI staining of hBMSCs in Fig. 4C indicated a homogenous distribution of actin fibers and filament elongation of cells on the scaffold. Additionally, as shown in Fig. 4D, hBMSCs were GFP-negative, distinguishing them from the GFP-positive HUVECs. In co-cultures, comparing the rhodamine phalloidin/DAPI staining image in Fig. 4E with the GFP fluorescent image in Fig. 4F, the distribution of hBMSCs in co-culture can be distinguished from that of GFP-tagged HUVECs. Contacting zones or overlapping growths were observed. Fig. 4G and H shows the F-actin staining of HUVECs and hBMSCs at a higher magnification, respectively. Obvious actin fiber bundles can be observed in the cytoplasm.

3.4. Immunofluorescent staining of PECAM-1

In HUVECs monocultures, immunofluorescent images show the expression of PECAM-1 at the cell–cell interface after 7 days of culture (Fig. 5). With increasing culture time, PECAM-1 expression of HUVECs became more pronounced and cells were observed forming network after 14 days. For both the 1:5 hBMSCs/HUVECs and HUVEC alone groups, PECAM-1 expression increased with culture time. The higher magnification images in the inserts showed the formation of small sprouts (Fig. 5). In the 5:1 and 1:1 hBMSC/HU-

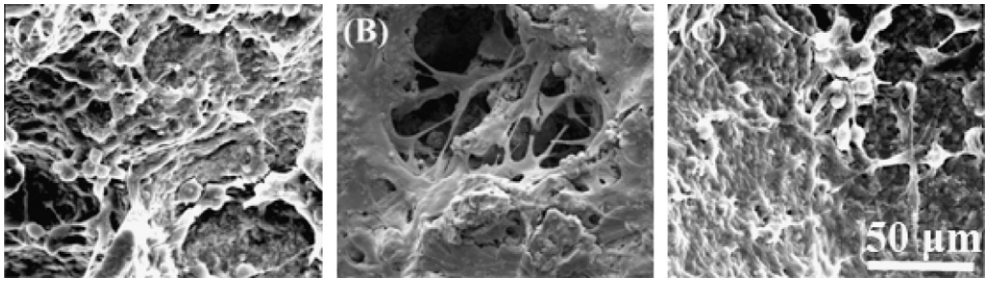

Fig. 3. Scanning electron micrographs showing cells growing on the β-TCP scaffolds after 3 days of culture: (A) HUVECs, (B) hBMSCs and (C) co-cultured hBMSCs/HUVECs (1:1 ratio).

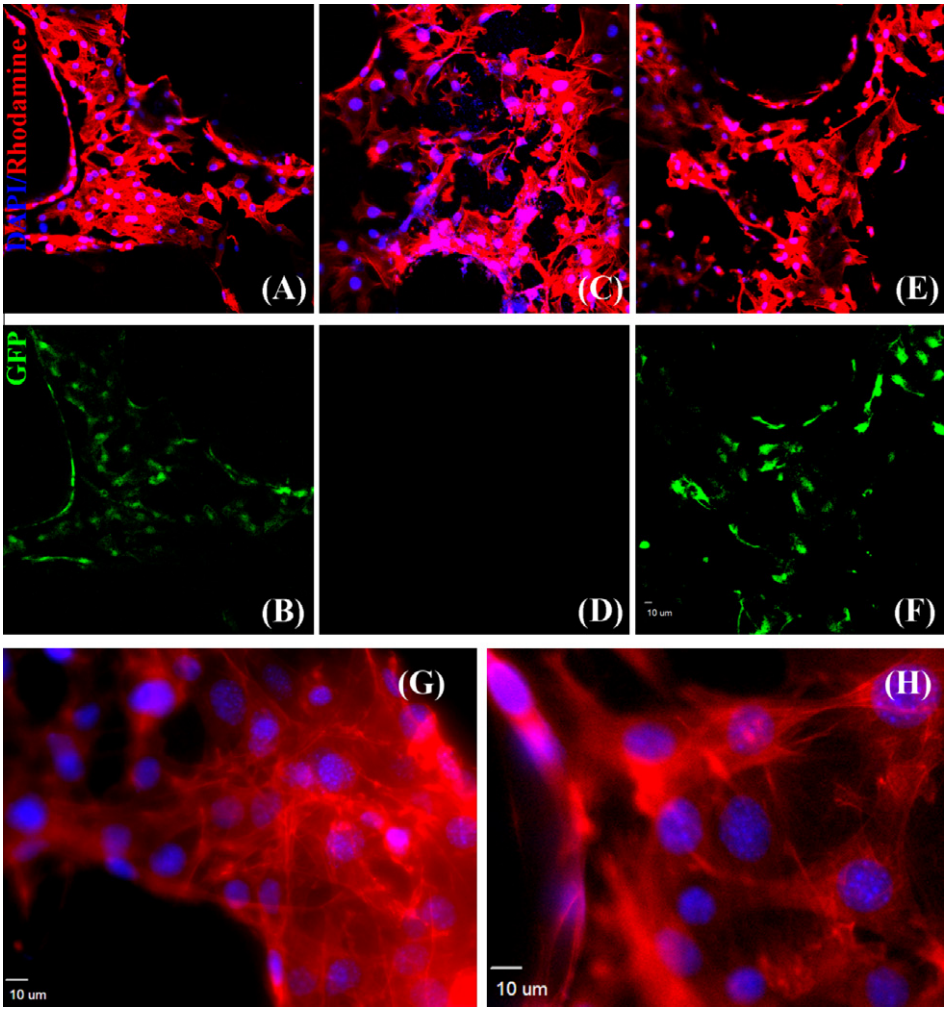

Fig. 4. Cytoskeletal organization of cells grown on the β-TCP scaffolds at day 7, as observed under a CLSM and demonstrated by rhodamine phalloidin/DAPI staining for F-actin/cell nuclei (A, C, E) and endogenous GFP (B, D, F). An abundance of F-actin fiber is observed in HUVECs (A, B), hBMSCs (C, D) and co-cultured hBMSCs/HUVECs (E, F), indicating a homogenous distribution of F-actin. (G) and (H) show F-actin staining of HUVECs and hBMSCs at a higher magnification, respectively.

VEC groups, these network structures were not apparent due to the lower proportion of HUVECs present.

3.5. Cell proliferation and ALP activity of hBMSCs

The proliferation of hBMSCs and HUVECs on the β-TCP scaffolds is shown in Fig. 6a. For hBMSC monocultures, cell proliferation increased from day 3 to day 7. After 7 days, cellular dsDNA content started to decrease. For HUVEC monocultures, cellular dsDNA amount increased from day 3 to day 14. The growth rate of HUVECs was slower compared to that of hBMSCs, but reached the same level of proliferation within 14 days of incubation. Compared to monocultures, the total cellular dsDNA amount in co-culture was proportional to the cell ratios and growth rates (Fig. 6a).

To evaluate the effect of HUVECs on the ALP activity of hBMSCs, hBMSCs were co-cultured with HUVECs at various ratios in non-osteogenic medium. The ALP activity of cells in monoculture and co-culture is shown in Fig. 6b. Results show that, in both mono- and co-culture, the ALP activity level of hBMSCs continually increased over 14 days (Fig. 6b). For the 5:1 and 1:1 hBMSC/HUVEC

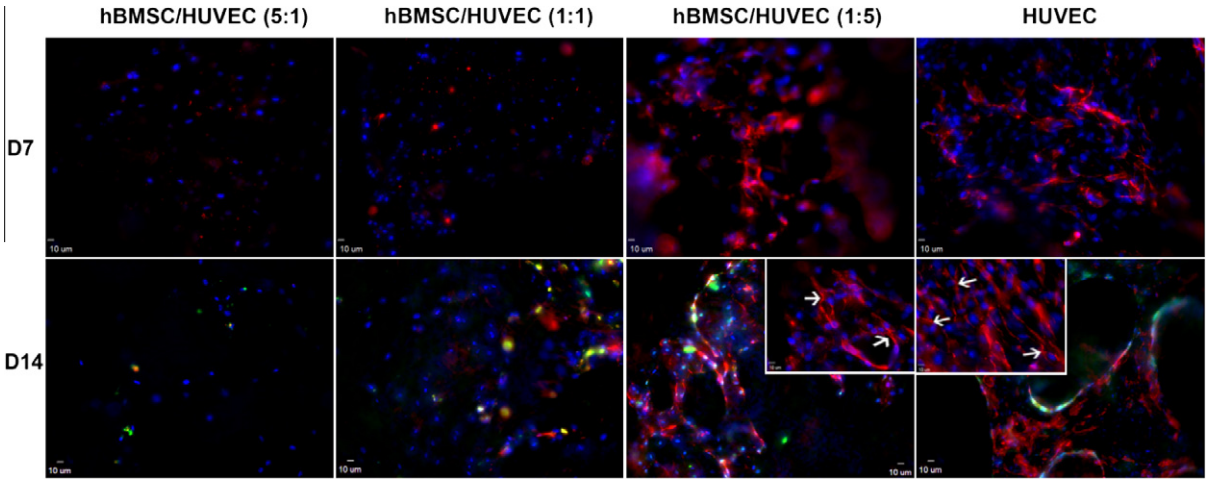

Fig. 5. CLSM images showing expression of endothelial marker, PECAM-1 (CD31), by HUVECs in monoculture and co-culture with hBMSCs at day 7 and day 14 on β-TCP scaffolds. Confocal images through a z-stack demonstrated the expression of CD31. Insert images represent CD31 expression of hBMSC/HUVEC (1:5) and HUVEC groups on day 14 at a higher magnification. Formation of small sprouts can be observed (white arrows). CD31 is in red (labeled with Alexa Fluor 594), and nuclei are in blue (labeled with DAPI).

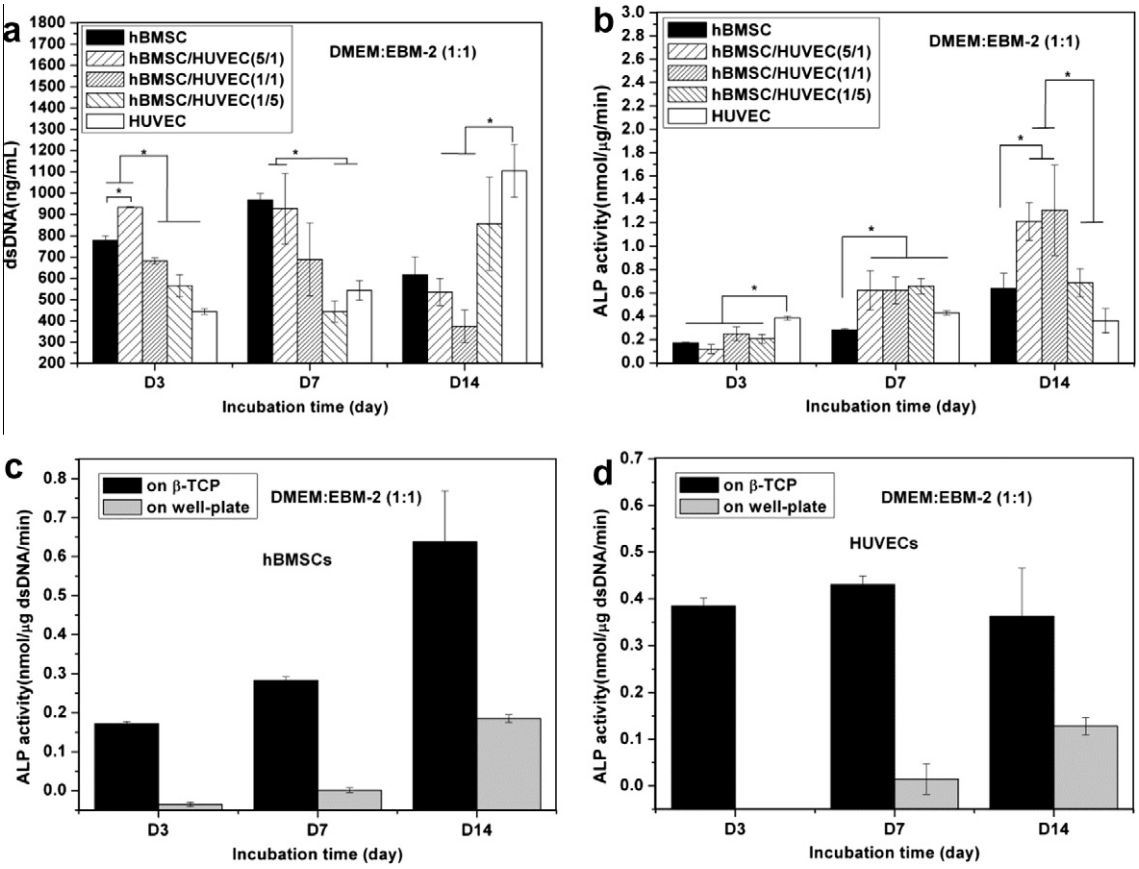

Fig. 6. dsDNA contents of cells in monocultured hBMSCs and HUVECs, and co-cultured hBMSCs/HUVECs at various ratios on the β-TCP scaffolds (a), and ALP activity expression in hBMSCs on the β-TCP scaffolds in monocultures and co-culture after 3, 7 and 14 days of incubation (b). ALP activity in monoculture hBMSCs (c) and HUVECs (d) on well plate and β-TCP scaffolds. An asterisk is used to indicate significant difference ($p < 0.05$).

groups, the ALP activity of co-cultured cells was significantly higher compared to those in monoculture ($p < 0.05$), except for the 1:5 hBMSC/HUVEC groups at day 14. ALP expression of HUVECs was higher than that in other groups at day 3, and it remained constant during 14 days of culture. ALP expression of hBMSCs or HUVECs alone on well plates was also investigated, and the results show that ALP activity could not be detected until day 14 (Fig. 6c and d), but the cells on the β-TCP scaffolds produced detectable ALP activity level at days 3 and 7 (Fig. 6b).

3.6. Gene expression

Quantitative real-time PCR was performed to evaluate the expression of osteogenic and endothelial markers. Fig. 7 shows

the osteogenic gene expression of hBMSCs and the endothelial gene expression of HUVECs in monoculture and co-culture. All gene expression was normalized to the expression levels of monocultured hBMSCs at day 7 (reference value set to 1).

For monocultures, the expression of *runx2* of hBMSCs did not change at 7 and 14 days of incubation. In the co-culture, *runx2* down-regulation increased with a decrease in the hBMSC/HUVEC ratio. *Alp* expression did not significantly change for monocultured hBMSCs, but it was significantly increased in the 5:1 hBMSC/HUVEC ratio group at day 7 and in the 5:1 and 1:1 hBMSC/HUVEC ratio groups at day 14. In monocultures, hBMSCs increased the expressions of *bsp* and *opn*, two early bone matrix genes, and reduced the expression of *oc*, a late bone matrix gene between day 7 and day 14 [31–33]. The addition of HUVECs significantly decreased the expression of the three genes in all co-culture groups. Additionally, these early osteogenic differentiation genes and bone matrix genes including *runx2*, *alp*, *bsp* and *opn* were detected at very low levels in HUVECs. In contrast, HUVECs expressed higher levels of *bmp-2* and *cd31*, when compared to hBMSCs. The expression of these two genes was detected in hBMSC monocultures. The expression of these two genes in co-culture groups increased as the hBMSC/HUVEC ratio decreased.

4. Discussion

β-TCP bioceramics have been widely used in clinical settings for bone repair and reconstruction [2,3]. In bone tissue engineering, it is common to merge biodegradable, biomimetic, porous CaP scaffolds with stem cells such as MSCs to regenerate bone tissue [4,8–11]. However, most of these works focused mainly on the osteogenic potential of MSCs on bioceramic scaffolds. It is well known that osteogenic and angiogenic processes are interdependent via the intimate interaction between bone-forming cells and endothelial cells [34–36]. An increasing number of studies have focused on the reciprocal effects between mesenchymal stem cells and endothelial cells or their corresponding precursors [37–40]. Although these studies provide new insights into the relationship between bone-forming cells and endothelial cells, the influence of the porous β-TCP ceramic scaffolds on the osteogenic and angiogenic potentials of hBMSCs and HUVECs in monoculture or co-culture is still not well understood.

In this study we investigated the cell behavior of HUVECs, hBMSCs and co-cultured hBMSCs/HUVECs on β-TCP scaffolds, including cell attachment, proliferation, and cell-specific marker expression. In co-culture, we mixed two types of cells in suspension and then seeded them on the β-TCP scaffolds. In this model, the interactions between two types of cells occurred by direct cell–cell contacts and diffusible paracrine signaling [38,41]. In these experiments, one major factor impacting cell behavior is the co-culture medium. Different culture media may lead to stem cell differentiation towards osteogenic, chondrogenic, endothelial, adipogenic and vascular smooth muscle phenotypes [42]. To select the appropriate co-culture medium in this study, we first co-cultured the two types of cells on well plates using three different media, including EBM-2, DMEM, and a 1:1 mixture of both. We found that the morphology of hBMSCs changed from spindle shape in DMEM to a slightly long, narrow spindle shape in EBM-2. In the mixture medium, the morphology of hBMSCs did not show this kind of change (S.1). For HUVECs, we found that they hardly survived or proliferated in DMEM. In a 1:1 mixture, the co-cultured cells can both display normal cell morphology as in their own preferred monoculture medium, regardless of their co-culture ratio (5:1, 1:1, 1:5; see S.1). To take into consideration the behavior of both cell types, the combined medium DMEM:EBM-2 (1:1) was selected to culture the cells on scaffolds. In this study, we were interested in the effect of β-TCP scaffolds on hBMSC and HUVEC monoculture and co-culture. Therefore, we used non-osteogenic medium in all experiments to exclude the medium effect on osteogenic activity level of hBMSCs.

The morphological observations by the confocal and SEM in Figs. 2 and 3 clearly indicate that the cells, in either monoculture or co-culture, can attach and proliferate well on the highly interconnected porous scaffolds. Cytoskeletal organization of cells on the scaffolds in Fig. 4 was also clearly observed. Cytoskeletal proteins such as actin have been used to illustrate spreading and attachment of cells on substrates [43]. Our F-actin labeling results show that HUVECs and hBMSCs exhibit uniform and homogenous distribution of actin in cytoplasm. These results indicate that the cells can attach and spread on the scaffolds. Previous studies have reported that biomaterial coated with extracellular matrix proteins significantly enhances attachment of endothelial cells to biomaterials and in some cases protein coating is a prerequisite for attachment of endothelial cells [20,44,45]. In this study, β-TCP scaffolds without pre-coating also supported attachment and spreading of endothelial cells.

The ALP activity level produced by hBMSCs on β-TCP scaffolds was significantly higher than that on well plates (Fig. 6c). This result implies that β-TCP scaffolds significantly promote early differentiation of hBMSCs. This may be attributed to the release of calcium and phosphate ions from β-TCP scaffolds. Our results indicated that Ca and P concentrations increased with the incubation time (S.3a). It has been indicated from previous studies that extracellular Ca^{2+} and inorganic P released by CaP biomaterials favor osteoblast differentiation, proliferation and matrix mineralization through activating Ca-sensing receptors in osteoblast cells [46–48]. Surprisingly, HUVECs seeded on β-TCP scaffolds also expressed ALP activity, although it remained constant over 14 days of incubation (Fig. 6b). Furthermore, HUVECs on well plates also exhibited ALP activity at day 14 (Fig. 6d). The HUVECs used in this study is a GFP transfected, immortalized cell line. The reason that HUVECs have a detectable ALP activity may be related to the mixture medium employed in this study or due to the release of Ca and P ions, which can alter the pH to a weak alkaline environment (S.3b). Alternatively, the change of pH from 7.4 to 7.9 due to the release of Ca and P ions may have induced ALP activity (S.3b). Wang et al. have also reported ALP expression in HUVECs in vitro [49]. Although the reasons remain unknown, it is clear that β-TCP scaffolds stimulated higher ALP activity in HUVECs on β-TCP scaffolds compared to those on well plates. This suggests that culture on a 3-D porous β-TCP bioceramic may change the behavior of HUVECs. More mechanistic studies to investigate the effects of 3-D structures on the morphology and calcium chemistry of cells should be performed to address these questions.

Our results further indicated that early ALP activities of the 5:1 and 1:1 co-culture groups were significantly higher than that of hBMSCs in monoculture. This may be a result of the BMP-2 secreted by HUVECs [49]. In real-time PCR, *bmp-2* gene expression was significantly higher in HUVECs when compared to hBMSCs, which further implies the possibility of HUVECs releasing soluble BMP-2 into the co-culture medium [49].

Additionally, the total dsDNA content of co-cultured cells was not the same as that of cells in monoculture, as shown in the dsDNA results (Fig. 6a). The proliferation rate of co-cultured mixture cells did not exceed that in monocultured hBMSCs but significantly exceeds that in monocultured HUVECs. This result could be explained by the dynamic change of percentage of both cell types in co-culture, as the growth rate of hBMSCs and HUVECs is different. hBMSCs grown in monoculture showed a clearly higher cell growth rate as compared with HUVECs in monoculture at an early stage (Fig. 6a). These results collectively suggested the interactions between hBMSCs and HUVECs in co-culture changed the individual growth rate of HUVECs and hBMSCs. This result further implied

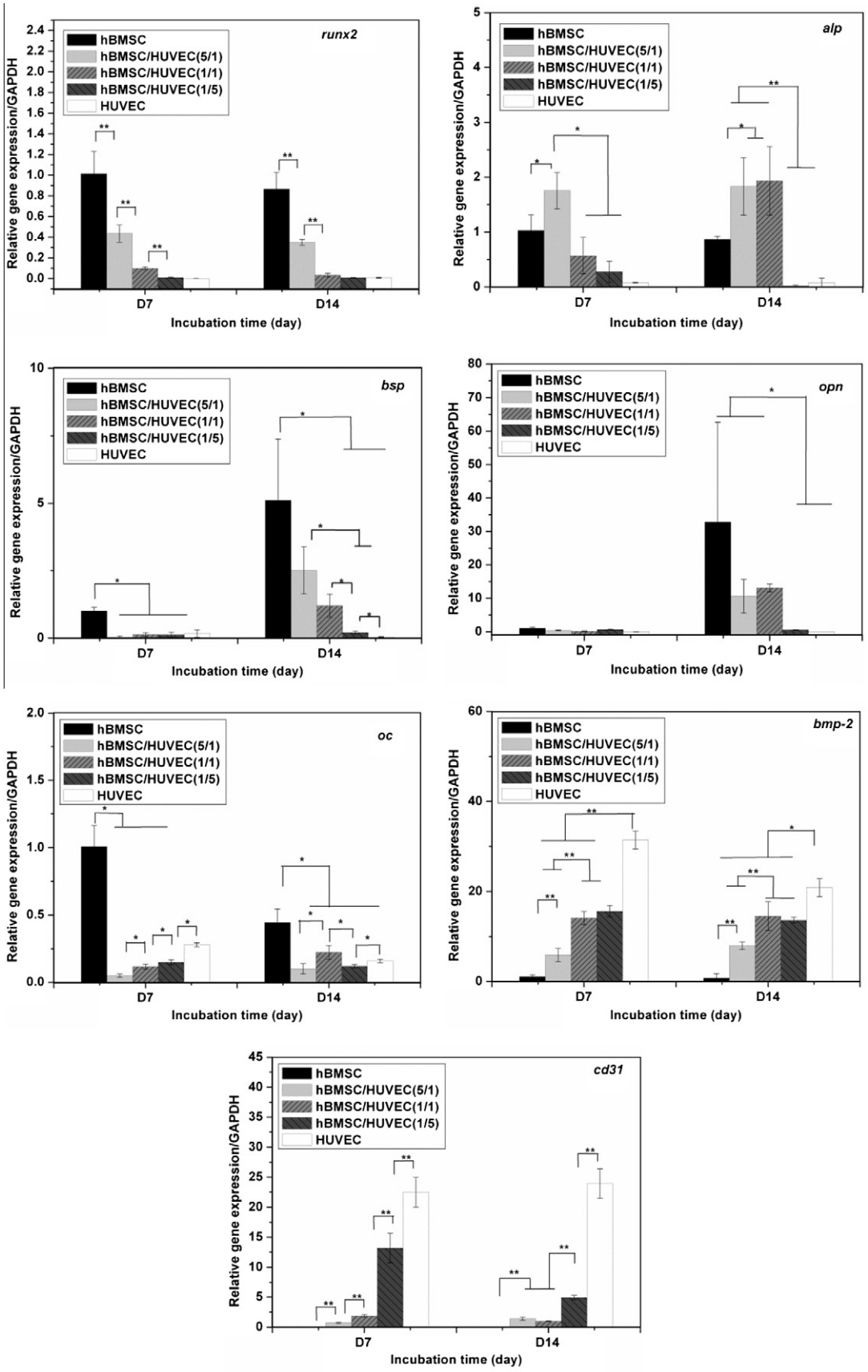

Fig. 7. Osteogenesis-related gene expression of hBMSCs on the β-TCP scaffolds in monoculture and co-culture after 7 and 14 days. One and two asterisks are used to show significant difference ($p < 0.05$ and 0.01, respectively).

that the HUVECs in co-culture may not stimulate hBMSCs proliferation; meanwhile, hBMSCs could suppress HUVEC expansion due to their high proliferative capacity in co-culture.

We further investigated the angiogenic potential of co-cultured cells in vitro on the β-TCP ceramic scaffolds. Cell adhesion molecule PECAM-1 expression at the cell–cell interface could be used to indicate the microcapillary-like structure or lumina. Cell adhesion molecule PECAM-1 expressed by HUVECs is known to be crucial for vessel formation and maintenance [50]. Our results show that in the HUVEC monoculture, a large amount of PECAM-1 expression can be clearly observed on the scaffolds shown in Fig. 5. Some elongated networks but no obvious lumina were observed during this experimental period. The ability of HVUECs to form lumina may depend on the properties of the extracellular matrix, which can affect the migration of HUVECs [51]. Co-culturing endothelial cells with bone-forming cells may facilitate the tube formation in vitro on scaffolds since the bone-forming cells can produce cytokines and angiogenic growth factors such as VEGF [52,53]. Also, the extracellular matrix produced by bone-forming cells may promote the formation of microcapillary-like structure when the cells co-cultured in direct contact [20,54]. Our data in co-culture did not show that hBMSCs promoted the tube formation of HUVECs on the scaffolds. Unlike the continuous PECAM-1 expression by the monocultured HUVECs at day 14 of incubation, a lower, scattered PECAM-1 expression can be observed in the groups of lower ratio of HUVECs (1:5 and 1:1). This is probably a result of decreased HUVEC population and the separation of HUVECs by hBMSCs. In the co-culture groups, hBMSCs and HUVECs were loaded simultaneously onto the porous scaffolds. A higher ratio of hBMSCs (5:1) in the mixed cell suspension could separate individual HUVECs, leading to the inability of HUVECs to contact and form a microcapillary-like structure.

The real-time PCR studies indicated that ALP gene expression levels in the co-culture group were significantly increased, but most of other genes were decreased. It is worth noting that we are unable to distinguish the contribution of individual cell type because gene expression in this study came from the total mRNA of two types of cells. As the expression level of hBMSCs is a part of the total expression level in the co-culture, therefore gene expression of all these osteogenic markers of hBMSCs specifically in co-culture could be higher [29]. Although further evaluation and new strategies will be needed to investigate the interactions between mesenchymal stem cells and endothelial cells on the biodegradable β-TCP, these present results implied that β-TCP scaffold with 3-D spatial features could be a useful platform to further investigate the interactions between the two cell types in 3-D structures for better understanding of bone regeneration, as this β-TCP ceramic scaffold can provide biocompatible and suitable surface properties for hBMSC and HUVEC development.

5. Conclusions

In the present study we examined the effect of an interconnected, macroporous, biodegradable β-TCP scaffold on cell behaviors of HUVECs and hBMSCs in both monoculture and co-culture. Our results demonstrate that β-TCP scaffolds supported the attachment and proliferation of HUVECs and hBMSCs in both monocultures and co-cultures. β-TCP scaffolds stimulated ALP activity of both hBMSCs and HUVECs. In co-cultures, HUVECs enhanced the very early osteogenic differentiation of hBMSCs. Meanwhile, the formation of an elongated network-like structure was observed in vitro on the β-TCP scaffolds. This β-TCP scaffold could provide a 3-D platform for studying interactions between multiple cells involved in bone regeneration. In particular, vascularization and osteogenesis of biodegradable β-TCP scaffolds can be promoted by manipulating structural and biological cues.

Acknowledgements

This work was supported by grants from the following agencies: NIH R01AR057837 (NIAMS), NIH R01DE021468 (NIDCR), DOD W81XWH-10-1-0966 (PRORP), W81XWH-10-200-10 (Airlift Research Foundation), W81XWH-11-2-0168-P4 (Alliance of Nano Health), and Wallace H. Coulter Foundation.

Appendix A. Figures with essential colour discrimination

Certain figures in this article, particularly Figs. 2, 4, and 5, are difficult to interpret in black and white. The full colour images can be found in the on-line version, at http://dx.doi.org/10.1016/j.actbio.2012.08.008.

Appendix B. Supplementary data

Supplementary data associated with this article can be found, in the online version, at http://dx.doi.org/10.1016/j.actbio.2012.08.008.

References

[1] Dietmar WH. Scaffolds in tissue engineering bone and cartilage. Biomaterials 2000;21:2529–43.
[2] Kalita SJ, Bhardwaj A, Bhatt HA. Nanocrystalline calcium phosphate ceramics in biomedical engineering. Mater Sci Eng C 2007;27:441–9.
[3] Descamps M, Duhoo T, Monchau F, Lu J, Hardouin P, Hornez JC, et al. Manufacture of macroporous [beta]-tricalcium phosphate bioceramics. J Eur Ceram Soc 2008;28:149–57.
[4] Pittenger MF, Mackay AM, Beck SC, Jaiswal RK, Douglas R, Mosca JD, et al. Multilineage potential of adult human mesenchymal stem cells. Science 1999;284:143–7.
[5] Chai YC, Roberts SJ, Desmet E, Kerckhofs G, van Gastel N, Geris L, et al. Mechanisms of ectopic bone formation by human osteoprogenitor cells on CaP biomaterial carriers. Biomaterials 2012;33:3127–42.
[6] Kasten P, Vogel J, Luginbühl R, Niemeyer P, Tonak M, Lorenz H, et al. Ectopic bone formation associated with mesenchymal stem cells in a resorbable calcium deficient hydroxyapatite carrier. Biomaterials 2005;26:5879–89.
[7] Kruyt MC, de Bruijn JD, Wilson CE, Oner FC, van Blitterswijk CA, Verbout AJ, et al. Viable osteogenic cells are obligatory for tissue-engineered ectopic bone formation in goats. Tissue Eng 2003;9:327–36.
[8] Arinzeh TL, Tran T, McAlary J, Daculsi G. A comparative study of biphasic calcium phosphate ceramics for human mesenchymal stem-cell-induced bone formation. Biomaterials 2005;26:3631–8.
[9] Dong J, Uemura T, Shirasaki Y, Tateishi T. Promotion of bone formation using highly pure porous β-TCP combined with bone marrow-derived osteoprogenitor cells. Biomaterials 2002;23:4493–502.
[10] Grynpas MD, Pilliar RM, Kandel RA, Renlund R, Filiaggi M, Dumitriu M. Porous calcium polyphosphate scaffolds for bone substitute applications in vivo studies. Biomaterials 2002;23:2063–70.
[11] Jafarian M, Eslaminejad MB, Khojasteh A, Mashhadi Abbas F, Dehghan MM, Hassanizadeh R, et al. Marrow-derived mesenchymal stem cells-directed bone regeneration in the dog mandible: a comparison between biphasic calcium phosphate and natural bone mineral. Oral Surg Oral Med O 2008;105:e14–24.
[12] Gerber HP, Vu TH, Ryan AM, Kowalski J, Werb Z, Ferrara N. VEGF couples hypertrophic cartilage remodeling, ossification and angiogenesis during endochondral bone formation. Nat Med 1999;5:623–8.
[13] Grellier M, Bordenave L, Amedee J. Cell-to-cell communication between osteogenic and endothelial lineages: implications for tissue engineering. Trends Biotechnol 2009;27:562–71.
[14] McCarthy I. The physiology of bone blood flow: a review. J Bone Joint Surg Am 2006;88(Suppl. 3):4–9.
[15] Rose FR, Cyster LA, Grant DM, Scotchford CA, Howdle SM, Shakesheff KM. In vitro assessment of cell penetration into porous hydroxyapatite scaffolds with a central aligned channel. Biomaterials 2004;25:5507–14.
[16] Ishaug SL, Crane GM, Miller MJ, Yasko AW, Yaszemski MJ, Mikos AG. Bone formation by three-dimensional stromal osteoblast culture in biodegradable polymer scaffolds. J Biomed Mater Res 1997;36:17–28.
[17] Rouwkema J, Rivron NC, van Blitterswijk CA. Vascularization in tissue engineering. Trends Biotechnol 2008;26:434–41.
[18] Smith MK, Peters MC, Richardson TP, Garbern JC, Mooney DJ. Locally enhanced angiogenesis promotes transplanted cell survival. Tissue Eng 2004;10:63–71.
[19] Klenke FM, Liu Y, Yuan H, Hunziker EB, Siebenrock KA, Hofstetter W. Impact of pore size on the vascularization and osseointegration of ceramic bone substitutes in vivo. J Biomed Mater Res A 2008;85:777–86.
[20] Unger RE, Sartoris A, Peters K, Motta A, Migliaresi C, Kunkel M, et al. Tissue-like self-assembly in cocultures of endothelial cells and osteoblasts and the formation of microcapillary-like structures on three-dimensional porous biomaterials. Biomaterials 2007;28:3965–76.

[21] Yu H, VandeVord PJ, Mao L, Matthew HW, Wooley PH, Yang SY. Improved tissue-engineered bone regeneration by endothelial cell mediated vascularization. Biomaterials 2009;30:508–17.
[22] Zhou J, Lin H, Fang T, Li X, Dai W, Uemura T, et al. The repair of large segmental bone defects in the rabbit with vascularized tissue engineered bone. Biomaterials 2010;31:1171–9.
[23] Liu Y, Kim JH, Young D, Kim S, Nishimoto SK, Yang Y. Novel template-casting technique for fabricating beta-tricalcium phosphate scaffolds with high interconnectivity and mechanical strength and in vitro cell responses. J Biomed Mater Res A 2010;92:997–1006.
[24] Kang Y, Kim S, Khademhosseini A, Yang Y. Creation of bony microenvironment with CaP and cell-derived ECM to enhance human bone-marrow MSC behavior and delivery of BMP-2. Biomaterials 2011;32:6119–30.
[25] Kang Y, Scully A, Young DA, Kim S, Tsao H, Sen M, et al. Enhanced mechanical performance and biological evaluation of a PLGA coated beta-TCP composite scaffold for load-bearing applications. Eur Polym J 2011;47:1569–77.
[26] Zhao J, Zhang N, Prestwich GD, Wen X. Recruitment of endogenous stem cells for tissue repair. Macromol Biosci 2008;8:836–42.
[27] Yim EK, Wan AC, Le Visage C, Liao IC, Leong KW. Proliferation and differentiation of human mesenchymal stem cell encapsulated in polyelectrolyte complexation fibrous scaffold. Biomaterials 2006;27:6111–22.
[28] Anderson JM, Vines JB, Patterson JL, Chen H, Javed A, Jun HW. Osteogenic differentiation of human mesenchymal stem cells synergistically enhanced by biomimetic peptide amphiphiles combined with conditioned medium. Acta Biomater 2011;7:675–82.
[29] Hofmann A, Ritz U, Verrier S, Eglin D, Alini M, Fuchs S, et al. The effect of human osteoblasts on proliferation and neo-vessel formation of human umbilical vein endothelial cells in a long-term 3D co-culture on polyurethane scaffolds. Biomaterials 2008;29:4217–26.
[30] Livak KJ, Schmittgen TD. Analysis of relative gene expression data using real-time quantitative PCR and the 2-[Delta][Delta]CT method. Methods 2001;25:402–8.
[31] Pham QP, Kurtis Kasper F, Scott Baggett L, Raphae RM, Jansen JA, Mikos AG. The influence of an in vitro generated bone-like extracellular matrix on osteoblastic gene expression of marrow stromal cells. Biomaterials 2008;29:2729–39.
[32] Sommer B, Bickel M, Hofstetter W, Wetterwald A. Expression of matrix proteins during the development of mineralized tissues. Bone 1996;19:371–80.
[33] Arafat MT, Lam CXF, Ekaputra AK, Wong SY, Li X, Gibson I. Biomimetic composite coating on rapid prototyped scaffolds for bone tissue engineering. Acta Biomater 2011;7:809–20.
[34] Kanczler JM, Oreffo RO. Osteogenesis and angiogenesis: the potential for engineering bone. Eur Cell Mater 2008;15:100–14.
[35] Towler DA. The osteogenic-angiogenic interface: novel insights into the biology of bone formation and fracture repair. Curr Osteoporos Rep 2008;6:67–71.
[36] Finkenzeller G, Arabatzis G, Geyer M, Wenger A, Bannasch H, Stark GB. Gene expression profiling reveals platelet-derived growth factor receptor alpha as a target of cell contact-dependent gene regulation in an endothelial cell-osteoblast co-culture model. Tissue Eng 2006;12:2889–903.
[37] Choong CS, Hutmacher DW, Triffitt JT. Co-culture of bone marrow fibroblasts and endothelial cells on modified polycaprolactone substrates for enhanced potentials in bone tissue engineering. Tissue Eng 2006;12:2521–31.
[38] Guillotin B, Bareille R, Bourget C, Bordenave L, Amedee J. Interaction between human umbilical vein endothelial cells and human osteoprogenitors triggers pleiotropic effect that may support osteoblastic function. Bone 2008;42:1080–91.
[39] Scherberich A, Galli R, Jaquiery C, Farhadi J, Martin I. Three-dimensional perfusion culture of human adipose tissue-derived endothelial and osteoblastic progenitors generates osteogenic constructs with intrinsic vascularization capacity. Stem Cells 2007;25:1823–9.
[40] Rouwkema J, de Boer J, Van Blitterswijk CA. Endothelial cells assemble into a 3-dimensional prevascular network in a bone tissue engineering construct. Tissue Eng 2006;12:2685–93.
[41] Villars F, Guillotin B, Amedee T, Dutoya S, Bordenave L, Bareille R, et al. Effect of HUVEC on human osteoprogenitor cell differentiation needs heterotypic gap junction communication. Am J Physiol Cell Physiol 2002;282:C775–85.
[42] Vater C, Kasten P, Stiehler M. Culture media for the differentiation of mesenchymal stromal cells. Acta Biomater 2011;7:463–77.
[43] Moghe PV, Berthiaume F, Ezzell RM, Toner M, Tompkins RG, Yarmush ML. Culture matrix configuration and composition in the maintenance of hepatocyte polarity and function. Biomaterials 1996;17:373–85.
[44] Unger RE, Huang Q, Peters K, Protzer D, Paul D, Kirkpatrick CJ. Growth of human cells on polyethersulfone (PES) hollow fiber membranes. Biomaterials 2005;26:1877–84.
[45] Unger RE, Peters K, Wolf M, Motta A, Migliaresi C, Kirkpatrick CJ. Endothelialization of a non-woven silk fibroin net for use in tissue engineering: growth and gene regulation of human endothelial cells. Biomaterials 2004;25:5137–46.
[46] Barradas AMC, Fernandes HAM, Groen N, Chai YC, Schrooten J, van de Peppel J, et al. A calcium-induced signaling cascade leading to osteogenic differentiation of human bone marrow-derived mesenchymal stromal cells. Biomaterials 2012;33:3205–15.
[47] Valerio P, Pereira MM, Goes AM, Leite MF. Effects of extracellular calcium concentration on the glutamate release by bioactive glass (BG60S) preincubated osteoblasts. Biomed Mater 2009;4:045011.
[48] Marie PJ. The calcium-sensing receptor in bone cells: a potential therapeutic target in osteoporosis. Bone 2010;46:571–6.
[49] Wang J, Ye Y, Tian H, Yang S, Jin X, Tong W, et al. In vitro osteogenesis of human adipose-derived stem cells by coculture with human umbilical vein endothelial cells. Biochem Biophys Res Commun 2011;412:143–9.
[50] Simon AM, McWhorter AR. Vascular abnormalities in mice lacking the endothelial gap junction proteins connexin37 and connexin40. Dev Biol 2002;251:206–20.
[51] Soucy PA, Romer LH. Endothelial cell adhesion, signaling, and morphogenesis in fibroblast-derived matrix. Matrix Biol 2009;28:273–83.
[52] Deckers MM, van Bezooijen RL, van der Horst G, Hoogendam J, van Der Bent C, Papapoulos SE, et al. Bone morphogenetic proteins stimulate angiogenesis through osteoblast-derived vascular endothelial growth factor A. Endocrinology 2002;143:1545–53.
[53] Furumatsu T, Shen ZN, Kawai A, Nishida K, Manabe H, Oohashi T, et al. Vascular endothelial growth factor principally acts as the main angiogenic factor in the early stage of human osteoblastogenesis. J Biochem 2003;133:633–9.
[54] Stahl A, Wenger A, Weber H, Stark GB, Augustin HG, Finkenzeller G. Bi-directional cell contact-dependent regulation of gene expression between endothelial cells and osteoblasts in a three-dimensional spheroidal coculture model. Biochem Biophys Res Commun 2004;322:684–92.